Nucleation Kinetics of *Cis*-Entacapone

D. Škalec Šamec,[a] E. Meštrović,[a] and A. Sander[b,*]
[a]PLIVA Croatia Ltd., Prilaz baruna Filipovića 25, 10000 Zagreb, Croatia
[b]University of Zagreb, Faculty of Chemical Engineering and Technology,
Marulićev trg 20, 10000 Zagreb, Croatia

The solubility curve and the metastable zone width for the system *cis*-entacapone – 2-propanol have been determined in defined process conditions. These results along with values of induction period for the constant feed concentration at different levels of supersaturation were used for evaluating interfacial energy according to the classical nucleation theory. The results obtained were used for calculation of the critical nucleus size, nucleation rate, and prediction of crystal growth mechanism.

Solubility data and metastable zone width determines the way to achieve the essential supersaturation level, as well as provides information necessary for control of the crystallization process. Knowledge of the fundamental parameters of nucleation kinetics led to the better understanding of the crystallization process in order to obtain a product with desired solid state characteristics.

Key words:
Crystal growth, entacapone, induction period, metastable zone width, nucleation, solubility

Introduction

Crystallization is a very complex separation process that involves simultaneous momentum, heat and mass transfer, and phase change. This process is used as a method of production, purification and a method of providing crystalline materials of desired crystal size distribution. In general, crystallization consists of two major steps, which take place simultaneously and can be independently controlled to a certain degree. The first step is the formation of nucleuses, and the second step is growth of crystals. Supersaturation is the main driving force for both steps. Supersaturation can be generated by cooling, evaporation, chemical reaction and by changing the solvent composition. Knowledge of the equilibrium curve is essential for selection of the appropriate method.[1–3]

Entacapone ((2*trans*)-2-cyano-3-(3,4-dihydroxy--5-nitrophenyl)-*N,N*-diethylprop-2-enamide) is a pharmaceutically active substance with two known isomers, *cis*-entacapone and *trans*-entacapone. The *trans*-isomer of entacapone was originally chosen because of a more favorable synthetic route. Both isomers are pharmacologically active as COMT-inhibitor and have equivalent activity.[4]

The aim of this research was to show the influence of additives on crystal morphology and evaluate the fundamental parameters of nucleation kinetics for crystallization of *cis*-entacapone from 2-propanol. This system was chosen among different organic solvents, due to the minimal influence of 2-propanol on the crystal morphology and good solubility of the chosen additive.[5] The external appearance of crystals obtained from an industrial crystallization process can have a major impact on a number of important properties relating to the slurry and the dry product. Crystal morphology will affect the rheological properties of the suspension, the filtration or centrifugation efficiency, the bulk density of the solid, and the flow properties of the solid. The control of crystal habit (along with crystal size distribution) is, therefore, an important part of the industrial crystallization processes. These results were determined by preliminary research of different crystallization methods such as evaporation, cooling and addition of antisolvent, which included variation of pressure, cooling rate, order and rate of addition of solvent/antisolvent regarding crystallization process (Fig. 1). The temperature range was selected to be as close to ambient conditions because of the future implementation in the process, which will be developed in line with the concept of green chemistry.

The metastable zone width and the induction period were determined. Based on the classical nucleation theory, interfacial energy was evaluated. The results obtained were used for calculation of the critical nucleus size, nucleation rate and prediction of crystal growth mechanism.

The product with desired solid-state properties depends on the well-defined and controlled crystallization process. Metastable zone width is a key parameter in these processes.

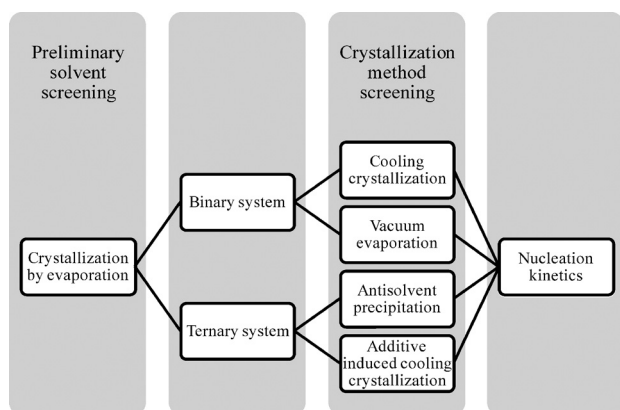*Corresponding author: asander@fkit.hr

F i g . 1 – *Research protocol*

Metastable zone width

The metastable zone is the region in the equilibrium (concentration – temperature) diagram between the solubility and supersolubility curve.[1–3] The metastable zone width is affected by a large number of factors, such as concentration, temperature, cooling rate, hydrodynamic conditions, presence of impurities or additives, and so on.[6–8] Data on the metastable zone width in desired process conditions (concentration, cooling rate, mixing rate,…) are important because they determine the granulometric properties of the obtained crystals.[1–3,9] At high levels of supersaturation, small crystals will be produced. On the other hand, lower levels of supersaturation usually results with larger crystals.

Today, various methods exist for measuring and predicting the metastable zone width.[8–16] The metastable zone width can be measured by the isothermal or polythermal method. The concentration of the solution can be determined indirectly by measuring the solution property that depends on temperature and concentration (density, conductivity, refraction index, turbidity...) or by the dry residue method.

Nucleation kinetics

Primary nucleation occurs mainly at high levels of supersaturation and predominates during unseeded crystallization.[1] If the supersaturated solution is clear, the stable nucleuses will be formed spontaneously (homogeneous nucleation). In the classical nucleation theory, the rate of homogeneous nucleation is given by an Arrhenius type of equation:[1–3]

$$B_0 = A \cdot \exp\left(-\frac{16 \cdot \pi \cdot \sigma^3 \cdot V_m^2 \cdot N_A}{3 \cdot R^3 \cdot T^3 \cdot (\ln S)^2}\right) =$$
$$= A \cdot \exp\left(-\frac{\Delta G_{cr}}{k_B \cdot T}\right) \qquad (1)$$

Superasturation is given by:

$$S = \frac{\gamma}{\gamma_S} \qquad (2)$$

Crystallization kinetics can be determined from the dependence between the induction period and the supersaturation. Induction period is the time between the creation of the initial supersaturation and the detection of the first formed crystals in the solution. Induction period is influenced by the level of supersaturation, solution properties, and process conditions. This period is usually measured by the previously mentioned isothermal method.

The induction period may be expressed as:

$$t_i = t_n + t_g \qquad (3)$$

With the assumption that steady-state nucleation is reached very quickly, and that the induction period is determined by the time needed for formation of the critical nucleus in the system and crystal growth, it can be written as:

$$t_i = A^{-1} \cdot \exp\left(\frac{16 \cdot \pi \cdot \sigma^3 \cdot V_m^2 \cdot N_A}{3 \cdot R^3 \cdot T^3 \cdot (\ln S)^2}\right), \qquad (4)$$

since:[1]

$$t_i \propto B_0^{-1} \qquad (5)$$

Induction period measurements are often used for evaluation of the interfacial tension.[17–23] For that purpose, eq. 4 is rewritten by taking logarithms to the following form:

$$\ln t_i = \ln A^{-1} + \left(\frac{16 \cdot \pi \cdot \sigma^3 \cdot V_m^2 \cdot N_A}{3 \cdot R^3 \cdot T^3} \cdot \frac{1}{(\ln S)^2}\right) \quad (6)$$

Interfacial tension can now be calculated from the slope, k, of the strait line (eq. 6):

$$\sigma = \sqrt[3]{\frac{3 \cdot R^3 \cdot T^3 \cdot k}{16 \cdot \pi \cdot V_m^2 \cdot N_A}} \qquad (7)$$

Critical nucleus size, r_c, can now be calculated from the Gibbs-Thomson equation:

$$r_c = \frac{2 \cdot \sigma \cdot V_m}{R \cdot T \cdot \ln S} \qquad (8)$$

The crystal growth mechanism was predicted from the values of the surface entropy factor, *f*, calculated by use of interfacial energy:[24]

$$f = \frac{4 \cdot V^{2/3} \cdot \sigma}{k_B \cdot T} \qquad (9)$$

Surface entropy factor indicates the roughness of the crystal surface. For:

$f < 3$:   rough interface and continuous growth

$3 < f < 5$:   birth and spread growth

$f > 5$:   very smooth crystal surface and spiral growth or screw dislocation.

Materials and methods

Materials

Mixture of toluene (Kemika Inc., Croatia), 3,4 – dihydroxy–5 –nitrobenzaldehyde (D'Orland KEG Ltd., Austria), 2-cyano-*N,N*-diethylacetamide (D'Orland KEG Ltd., Austria) and piperidine acetate (synthesized from piperidine (Sigma Aldrich Chemie Ltd, Germany), Glacial acetic acid (Sigma Aldrich Chemie Ltd, Germany) and toluene) was stirred at reflux temperature. Reaction mixture was cool down to RT. Acetone (Kemika Inc., Croatia) and hydrochloric acid (Kemika Inc., Croatia) was added. The obtained crystals were filtered off and rinsed with toluene.[25] The filtrate containing *cis*-isomer of entacapone was concentrated and crystallized from toluene/methanol (Kemika Inc., Croatia) mixture. The obtained crystals were filtered off and dried.

Preliminary solvent screening

50 mg of *cis*-isomer of entacapone was dissolved by heating at reflux temperature (boiling point temperature) in required volume of solvent. The prepared solution was left in an open vessel at room conditions until first crystals were formed due to the solvent evaporation.

Binary systems (API/solvent)

Vacuum evaporation

100 mg of *cis*-isomer of entacapone was dissolved at room conditions in a previously determined volume of selected solvents. The solution was filtrated into a round flask (50 cm³). The solvent was evaporated at room temperature and different pressures (100, 500 and 800 mbar) in a rotary evaporator at the rotational speed of 50 rpm (Buchi). The influence of the pressure on crystal morphology was analyzed.

Cooling crystallization

Saturated solutions (313 K for 1,2-dichloromethane; 323 K for other solvents) of *cis*-isomer of entacapone and selected solvents were prepared in a round flask (100 cm³) equipped with mechanical stirrer (100 rpm), condenser and thermostat/ice bath (according to required cooling rate). The obtained solution was cooled down to 283 K at three different cooling rates. The influence of the cooling rate on crystal morphology was analyzed.

Ternary systems

Antisolvent precipitation

Two different sets of experiments were conducted according to the sequence of addition: antisolvent to solution; solution to antisolvent. The volume ratio of solution to antisolvent was always the same, 1:2. 100 mg *cis*-isomer of entacapone was dissolved at 293 K in selected solvent. For the first set of experiments, the solution was poured into a round flask (100 cm³) equipped with mechanic stirrer (100 rpm) and peristaltic pump/addition funnel. Antisolvent was added at different rates. In the second set of experiments, the antisolvent was poured into a round flask and solution was added at the defined rate. Suspension was stirred for an additional 5 minutes after antisolvent or solution was added. The influence of the type of solvent or antisolvent, sequence of addition, and rate of addition was analyzed.

Additive-induced crystallization

The defined amount of *cis*-isomer entacapone was dissolved in 200 cm³ of 2-propanol by heating in reactor (250 cm³, equipped with condenser, mechanical stirrer (200 rpm), turbidimetric probe and thermostat). *Trans*-isomer of entacapone (additive) was added into the solution, which was then heated 10 K above the saturation temperature and stirred for 15 minutes. The solution was cooled down (1 K min⁻¹) and crystallization was observed by turbidimetric probe.

Nucleation kinetic

Measurement of solubility

Solubility of *cis*-entacapone in 2-propanol (Merck, Germany) was measured at three temperatures ranging between 298 and 308 K. *cis*-entacapone was added in excess and agitated for 24 hours in a thermostated vessel.[26] The suspension was then filtered and the concentration of the solution measured by means of liquid chromatography method (HPLC 1100, Agilent Technologies, USA).

Metastable zone width measurement

The prepared solutions of *cis*-entacapone in 2-propanol were heated to 10 K above the saturation temperature, mixed for 15 minutes, and then cooled down at the controlled rate of 1 K min⁻¹.[27] Crystallization process was monitored by a turbidimetry method using Trb8000, Mettler Toledo, USA and turbidimetry probe InPro 8200/S(H).

Measurement of induction time

The induction time was determined by the isothermal method.[28] Prepared solutions of *cis*-entacapone in 2-propanol were heated to 343 K, and then rapidly cooled to the temperature that corresponds to the required supersaturation. This supersaturation was maintained until the first crystals were observed.

Powder characterisation

X-ray analysis of the obtained crystals was carried out in a Philips X'Pert PRO diffractometer (Philips, Holland) using Cu Kα radiation over a 2θ range between 4 and 40° with an operating potential of 45 kV, a current of 40 mA, while the goniometric step was 0.016 degrees. Sampling time was 100 s. The obtained diffractograms were analyzed by means of X'Pert Graphics and Identify software, Philips Analytical, Holland.

Particle morphology

The morphology of crystals was determined by scanning electron microscope JSM-5800 (JEOL, Japan) using software LINKISIS, Oxford Instruments, UK. Images were analyzed by software IMQuant, Oxford Instruments, UK. Values of Aspect Ratio were calculated as ratio between the smallest and largest side of crystal, which were measured by software AnalySIS, Olympus, USA.

Results and discussion

Initial solvent screening

In order to define the most appropriate system and crystallization method for crystallization of *cis*-entacapone, different types of solvents, antisolvents, additives and methods for generating supersaturation were investigated in laboratory scale, as presented on Fig. 1. Initial solvent screening resulted with the selection of six different solvents (acetone, 1,2-dichloromethane, ethanol, ethyl acetate, ethyl methyl ketone and 2-propanole) and three antisolvents (cyclohexane, *n*-heptane and petrol ether). Among 87 tested solvents, those whose solubility of *cis*-entacapone was higher than 25 g dm^{–3} were selected as solvents.[5] On the other hand, solvents whose solubility of *cis*-entacapone was lower than 5 g dm^{–3} were selected as antisolvents.

The next step was the selection of the most suitable system for crystallization of *cis*-entacapone based on the morphology of the obtained crystals. The goal was to find the system with the highest insensitivity of the crystal habit to the proc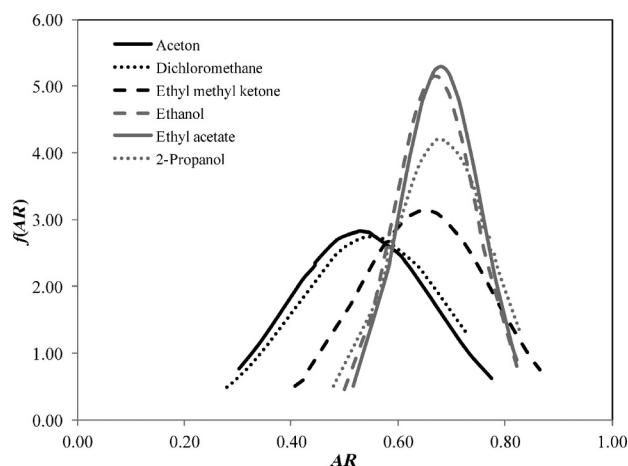ess conditions. For that purpose, three crystallization methods were employed: vacuum evaporation, cooling crystallization and antisolvent precipitation. The obtained crystals were characterized by aspect ratio. The results were systemized by used solvent and results for each group were shown as Gaussian distribution (Fig. 2). Aspect ratio and Gaussian distribution were calculated by the following equations:

F i g . 2 − *Gaussian distributions (vacuum evaporation, cooling crystallization and antisolvent precipitation under various process conditions for different solvents)*

$$\overline{AR} = \frac{1}{n} \cdot \sum_{i=1}^{n} AR_i \qquad (10)$$

$$f(AR) = \frac{1}{n\pi\sigma^2} \cdot \exp\left(-\frac{(AR - \overline{AR})^2}{2\sigma^2}\right) \quad (11)$$

Results of Gaussian distribution showed that ethanol, ethyl acetate and 2-propanol have the narrowest distribution. In other words, crystals obtained by these solvents, regardless of the crystallization method and process conditions, will have similar habit.

Finally, the most appropriate solvent was selected based on the crystal yield and the solubility of additive in these three solvents. Crystallization efficiency expressed as the crystal yield for all three solvents and different crystallization methods is presented in Table 1.

Crystal yield is defined by:

$$\text{Yield} = \frac{m_i}{m_c} \qquad (12)$$

When supersaturation was induced by vacuum evaporation, only two systems resulted in crystallization: *cis*-entacapone − 2-propanole and *cis*-entacapone − ethanol. Aspect ratio and the maximal crystal size, as well as the crystal size interval are all increased by the increase in operating pressure.

T a b l e 1 – *Crystal yield and size intervals obtained with different crystallization methods*

	Process condition range	2-propanole			Ethanol			Ethyl acetate		
		yield, %	x_{min}, μm	x_{max}, μm	yield, %	x_{min}, μm	x_{max}, μm	yield, %	x_{min}, μm	x_{max}, μm
Vacuum evaporation	Pressure, mbar:									
	100	61	24	156	58	98	456			
	500	56	26	180	50	206	576	without crystallization		
	800	53	26	257	36	190	654			
Cooling crystallization	Cooling rate, K min^{-1}									
	0.2	73	12	115	68	65	246	55	7	98
	1.0	69	17	110	73	42	213	40	4	69
	6.0	75	23	98	68	14	91	52	3	51
Antisolvent precipitation with cyclohexane	Antisolvent addition rate, cm^3 min^{-1}									
	0.2	56	15	172	48	8	36	40	8	39
	0.5	64	17	139	40	16	38	62	9	45
	1.5	66	21	137	42	17	32	50	12	36
	Solvent addition rate, cm^3 min^{-1}									
	0.3	38	18	128	42	10	46	38	7	45
	1.0	50	25	124	58	21	43	71	9	35
	15.0	50	24	119	40	10	26	28	13	29

At lower pressure, nucleation is enhanced due to the higher supersaturation induced by higher driving force, and consequently resulted with the higher crystal yield. Since the supersaturation was spent mostly on the nucleation step, final crystals are smaller. At lower operating pressure, the boiling point of solvent is reduced, so it will easily evaporate and the supersaturation will be generated faster. At higher operating pressure, supersaturation was generated slowly, so fewer nucleuses were formed and supersaturation was spent on crystal growth. Larger crystals were obtained with ethanol as the solvent, so the crystal growth rate was higher.

Increase in cooling rate results with intense supersaturation, and in the similar way influences the crystallization kinetics as the decrease of operating pressure. Again, crystal growth was faster for the system *cis*-entacapone – ethanol. From the solution of *cis*-entacapone – ethyl acetate nucleation occurred at the highest rate since the obtained crystals have the smallest size.

For the antisolvent precipitation, the highest nucleation and crystal growth rates were obtained for the solution of *cis*-entacapone in 2-propanole. For that system, the highest crystal yield was obtained when cyclohexane was used as antisolvent. Therefore, these experimental data are presented in Table 1. When antisolvent is added to the solution, an increase in the addition rate causes a decrease in maximal crystal size since nucleation is enhanced due to the higher supersaturation level. On the other hand, crystallization time is shorter because additive was added faster while additional mixing time was the same for all experiments. Smaller crystals were obtained when the order of addition was changed. Increase in addition rate caused higher supersaturation degree, higher nucleation rate, and finally smaller final crystal size. Both nucleation and crystal growth rates were lower for the other two systems of investigated solvents and antisolvents.

The results show that process parameters such as pressure, cooling rate, adding rate and order of adding antisolvent or solution do not affect significantly the morphology of *cis*-isomer of entacapone, regardless of the fact that these process parameters influence supersaturation. From the above results, it can be concluded that 2-propanole is the most suitable solvent for further investigations.

Since the majority of crystals are agglomerated, as it will be presented in the section about crystal morphology, the influence of additives were analyzed. For that purpose, all other process parameters, including solvents, must have minimum effect on morphology. In addition, the additive must be soluble in the selected solvent in order to assure that the conditions for the homogeneous nucleation are fulfilled. If the additive is not soluble in solvent,
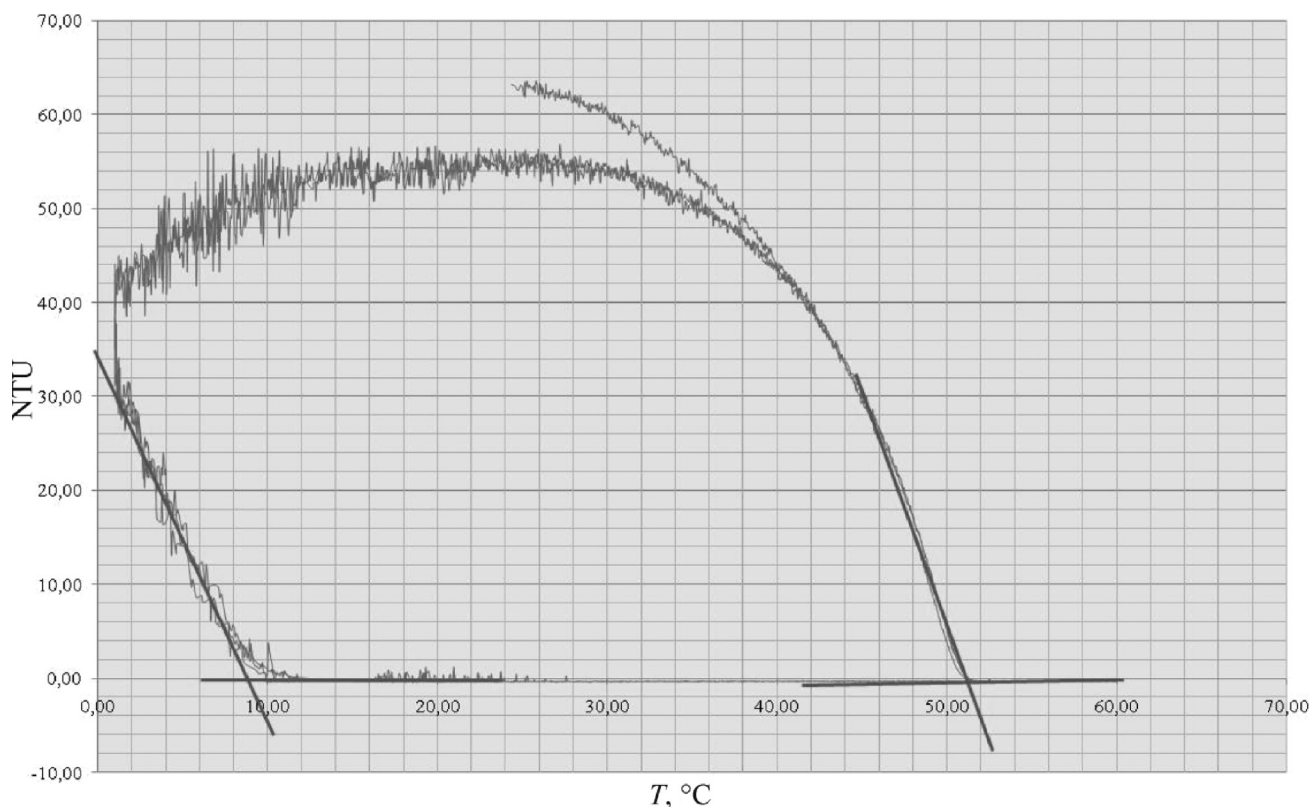
F i g . 3 – *Change in turbidity during measurements of the metastable zone width*

then it will act as an impurity, so heterogeneous nucleation will occur. Again, ethanol, ethyl acetate and 2-propanole were the best candidates due to the narrowest Gausian distributions. *Trans*-entacapone was selected as an additive since it has the same pharmaceutical activity as *cis*-isomer of entacapone, and is commercially available. Moreover, no further toxicological study is necessary in the case it cannot be eliminated from the final product. The solubility of *trans*-entacapone in 2-propanole was higher (50 g dm^{-3}) than in the other two solvents (25 g dm^{-3}), so the selection of 2-propanole as the most suitable solvent was confirmed.

Metastable zone width

Metastable zone width was determined for the solution of *cis*-isomer entacapone in 2-propanol in order to define temperature range in which additive can be added.

Solubility and supersolubitiy curves are critical parameters for the definition of the operational limits for crystallization process, and provide information on the maximum theoretical yield for a given system.[8] The metastable zone width was determined from the turbidity measurements during the cooling and heating cycles of the solutions of defined concentrations. Many authors use this method for measuring the metastable zone width, since the method

precisely detects the cloud and clear points during nucleation and dissolution of crystals.[10,11,15,16] Turbidity is considered a good measure of the degree of the solution transparency due to the presence of suspended particles. Measurements were repeated three times for all concentrations. Fig. 3 shows the dependence of the turbidity on solution temperature for concentration of *cis*-entacapone equal to 20 g dm^{-3}. The metastable zone width, *MZW*, was calculated from temperatures at which the linear parts intersect the *x*-axis.

$$MZW = T_{ss} - T_s \qquad (13)$$

Fig. 4 shows the metastable zone width for *cis*-entacapone – 2-propanol system, in given process conditions of cooling and mixing. As expected, the solubility of *cis*-entacapone in 2-propanol increases with temperature. The metastable zone width becomes slightly narrower at higher temperatures. Due to a higher concentration of *cis*-entacapone in solution, a lower driving force for crystallization is needed. In other words, a critical nucleus can be formed easier since lower energy barriers must be exceeded. During crystallization, the formation of nucleuses and their dissolution occurred continuously at the same time. In diluted solutions, dissolution predominates, while at higher concentrations the solution consists of a higher amount of solute ready to incorporate into the crys-
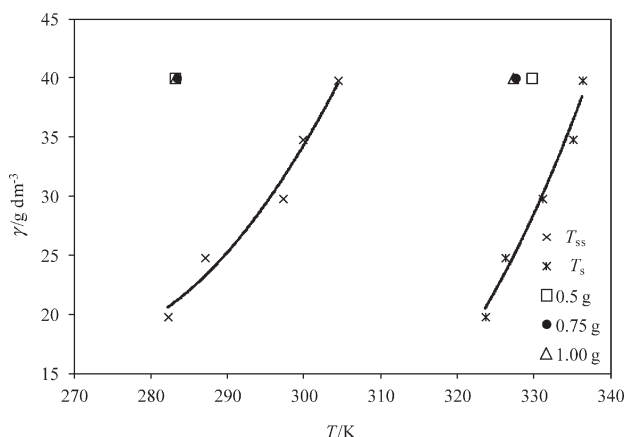
F i g . 4 – *Metastable zone width for the system cis-entaca-pone – 2-propanol*

T a b l e 2 – *Fundamental parameters of nucleation of cis-entacapone in 2-propanol*

T, °C	γ, g dm^{-3}	t_i, min	S	σ, mJ m^{-2}	r_{cr}, nm	ΔG_{cr}, kJ mol^{-1}	B_0, Nuclei m^{-2} min^{-1}
301.25	40	52	24.75	12.19	0.646	12.85	0.147
303.95	40	90	22.25	12.30	0.669	13.87	0.136
307.65	40	114	19.90	12.45	0.694	15.11	0.071

tal lattice, so lower levels of supersaturation are needed for formation of a stable critical nucleus.

The metastable zone width is wide enough for selection of the conditions for crystallization of *cis*-entacapone form 2-propanol of the desired crystal sizes.

Solubility and supersolubility curves in the investigated ranges of temperatures can be calculated from the following equations:

$$\gamma_s = 0.0257 \cdot T^2 - 15.52 \cdot T + 2355.3 \quad (14)$$

$$\gamma_{ss} = 0.0176 \cdot T^2 - 9.462 \cdot T + 1290.7 \quad (15)$$

In order to study the influence of additives on the metastable zone width and crystal morphology, a different amount of *trans*-entacapone was added to the solution of *cis*-entacapone in 2-propanole (0.50, 0.75, 1.00 % in relation to amount of *cis*-isomer of entacapone). Initial concentration of *cis*-entacapone was 40 g dm^{-3}. It can be seen from Fig. 4 that *trans*-entacapone increases the solubility and supersolubility of *cis*-entacapone. The metastable zone width was wider. Due to the wider metastable zone, crystallization will occur at lower temperatures and consequently the nucleation will be enhanced due to the higher driving force.

Nucleation kinetics

Induction period was measured for the constant feed concentration of 40 g dm^{-3} at different levels of supersaturation. Since at higher supersaturation, when the solution was cooled to a lower temperature, the formation of nucleuses was enhanced, the induction period was shorter (Table 2). Therefore, the induction period is influenced by the supersaturation and temperature.[21–23,27–29] In order to determine the interfacial tension, the solubility of *cis*-entacapone in 2-propanol was measured in the narrow temperature range between 301 and 308 K.

This range was chosen because the aim was to develop green chemistry processes, with one of its principles for obtaining maximum energy efficiency by conducting a process such as crystallization in ambient conditions.[30] The obtained results are shown in Fig. 5. In this low temperature range, the solubility curve exhibits a quite different trend. Both, *cis*-entacapone and 2-propanol are able to form hydrogen bonds. The concentration of solute influences the arrangements of the molecules present in the solution and consequently the hydrogen bonds network. A substantial number of noncovalent interactions working together are necessary to hold the structures together. It is possible that at different concentrations, different hydrogen bond networks are formed resulting in changes in the slope of the solubility curve.
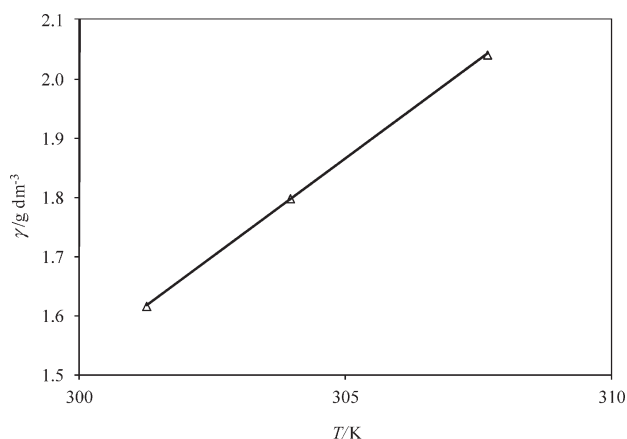

F i g . 5 – *Solubility of cis-entacapone in 2-propanol*

According to eq. 6, the plot $\ln t = f(\ln^{-2} S)$ was constructed (Fig. 6). Interfacial energy was calculated (eq. 7) and presented in Table 2. Interfacial energy increases with the increase of temperature and the decrease of supersaturation. Generally, interfacial energy is influenced by temperature, the nature of the liquid and surrounding environment, the crystal structure, and the surface plane. The degree of probability of nucleation depends on the molecular distances of the solute in the solution. At higher concentrations, the molecules are closer to
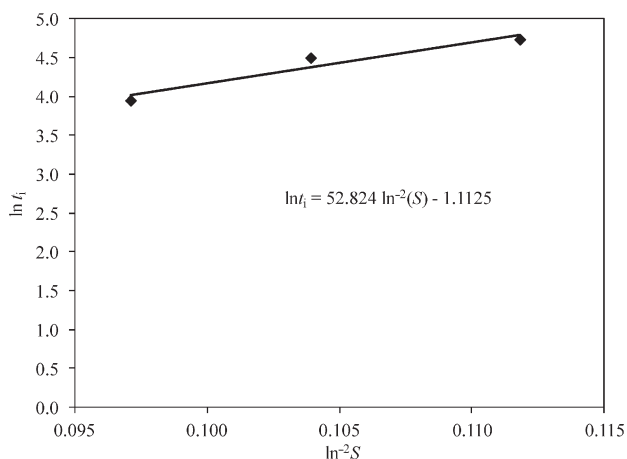
F i g . 6 — *Plot of ln(t) = f(ln^{-2}S)*
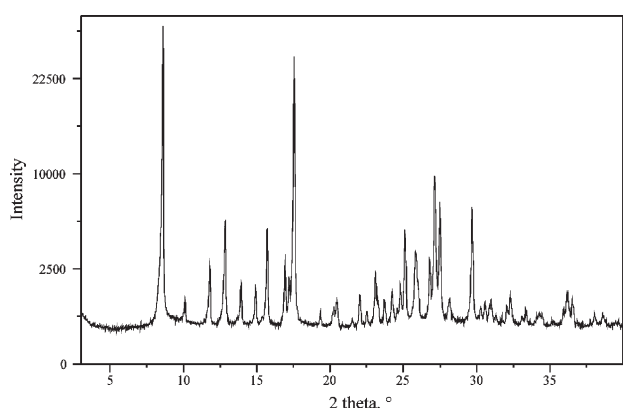
F i g . 7 — *XRD pattern of cis-entacapone*

each other in the solution, so nucleation is easier, the critical nucleus size smaller, and finally lower Gibbs free energy is needed. The formation of new phase (crystal) from the solution requires the creation of an interface between two phases. This is followed by the energy consumption, which depends on the interfacial energy. A molecule on the crystal surface has fewer bonds than a molecule within the crystal bulk. Energy difference per molecule on the surface and within the bulk depends on the arrangement of molecules on the crystal surface and in the crystal bulk. Interactions of molecules present in the solution, at or near the surface, are responsible for different rearrangement of structures in the surface layers. Due to different degrees of unsaturation of bonds on the crystal surface, different amounts of energy are needed for creation of a unit area of interface.

The influences of temperature and supersaturation ratio, S, on the interfacial energy (in the investigated ranges of temperature; and solute concentration 40 g dm^{-3}) are given with the following equations:

$$\sigma = 0.0405 \cdot T \qquad (16)$$

$$\sigma = -0.0533 \cdot S + 13.506 \qquad (17)$$

Nucleation rate was calculated (eq. 1), with the data obtained from the induction period measurement (slope and intercept of $\ln t = f(\ln^{-2} S)$). Nucleation rate is lower at higher temperature and lower supersaturation due to higher energy requirements for creation of stable nucleuses.

Calculated value of surface entropy factor was the same for all experiments ($f = 3.69$). Since the surface entropy factor is larger than 3, the crystal growth is controlled by birth and spread, which in turns results with smoother crystal faces.[24] The energy barrier for growth of *cis*-entacapone from 2-propanol is high enough to hinder the continuous growth of nucleuses and to decrease the crystal growth rate. Usually, at high growth rates rougher crystal surfaces evolved.
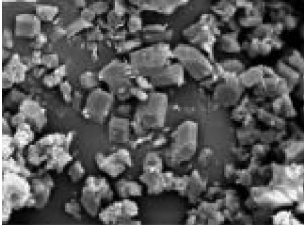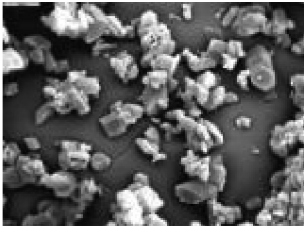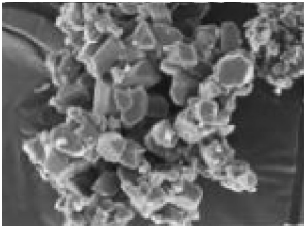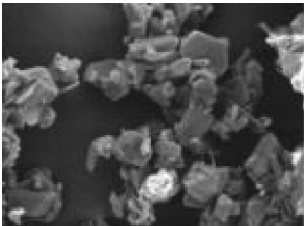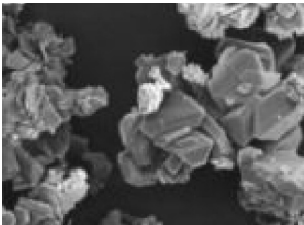
Characterization and morphology of the obtained crystals

Crystals obtained during cooling crystallization are shown in Table 3. Concentration of the solution slightly influences the crystal morphology. Higher supersaturation levels at lower concentrations resulted in higher nucleation rates and formation of larger numbers of nucleuses, thus obtaining smaller crystals. Aspect ratio, *AR*, has slightly lower values at higher temperatures. This means that the crystal growth rate in one direction is higher, and consequently the crystals are more elongated. Agglomeration is more pronounced at the higher solution concentration.

Crystals obtained by different crystallization method are presented in Table 4. As mentioned earlier, when supersaturation was generated by vacuum evaporation or cooling, only slight changes in crystal morphology could be observed. Crystals obtained by vacuum evaporation have extremely irregular shape and most of them are agglomerated. This happens probably as the result of improper mixing conditions in the rotary evaporator. Agglomerated crystals were also obtained by cooling crystallization, even though some individual larger crystals can be observed at lower cooling rates. At the highest cooling rate, all crystals are agglomerated. High supersaturation levels pronounce nucleation. Large number of small crystals will easily form agglomerates due to the attractive electrostatic forces.

When antisolvent was added to the solution of *cis*-entacapone, agglomeration was more pronounced at the lowest addition rate. In such conditions, the time needed for addition of antisolvent was the longest. During that time, supersaturation constantly varied, and nucleation was simultaneously induced. The fraction of new small nucleuses constantly increased so again agglomeration

T a b l e 3 – *Morphology of the obtained crystals*

γ, g dm^{-3}	T_s, K	T_{ss}, K	ΔT, K	AR	SEM image enlargement: 1000 x
19.8	323.65	282.25	41.4	0.70	
24.5	326.25	287.07	39.18	0.68	
29.8	331.10	297.25	33.85	0.68	
34.8	335.08	299.83	35.25	0.62	
39.8	336.32	304.43	31.89	0.63	

was pronounced. Higher degree of morphology changes could be observed when solution was added to the antisolvent. Agglomerates consist of larger crystals. Small amount of solvent is in contact with large amount of antisolvent. This results with the formation of a smaller number of nucleuses, which are allowed to grow before another amount of solvent is added.
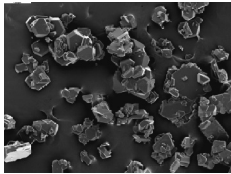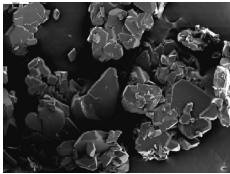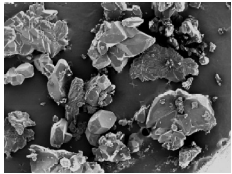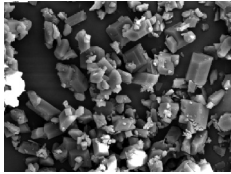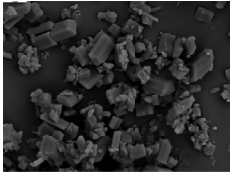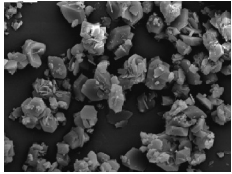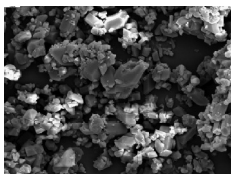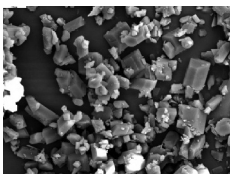
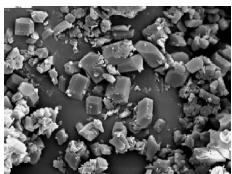When *trans*-entacapone, as an additive, was added to the solution, the agglomeration was suppressed even though the supersaturation level was increased. The obtained crystals were elongated (small aspect ratio), so unwanted crystal morphology was obtained.

The obtained crystals were characterized by means of XRD. Typical difractogram of *cis*-entacapone is shown in Fig. 7.

Conclusions

After initial solvent screening, three solvents (ethyl acetate, 2-propanol and ethanol) with the narrowest aspect ratio distribution were selected. Based on the morphology of crystals obtained by different crystallization methods and crystal yield, 2-propanole was chosen as the best candidate. From the obtained results for crystallization of

T a b l e 4 – *Morphology of crystals obtained by different crystallization methods (system cis-entacapone – 2-propanole)*

Crystallization method	p, mbar	100	500	800
Vacuum evaporation				
	AR	0.77	0.78	0.83
	CR, K min^{-1}	0.2	1.0	6.0
Cooling crystallization				
	AR	0.69	0.77	0.67
	V_a, cm^3 min^{-1}	0.2	0.5	1.5
Antisolvent precipitation cyclohexane				
	AR	0.73	0.78	0.71
	V_s, cm^3 min^{-1}			
		0.3	1.0	15.0
	AR	0.58	0.75	0.79
	x, %	0.50	0.75	1.00
Additive induced crystallization				
	AR	0.28	0.30	0.25

cis-entacapone from 2-propanole solution, it can be concluded that the crystallization method and the process conditions (pressure; cooling rate; order and rate of addition) do not significantly influence crystal morphology. Agglomeration was suppressed when crystallization was induced by addition of *trans*-entacapone, but crystals of unwanted habit (elongated crystals) were obtained. Since the highest crystal yield was observed for cooling, crystallization nucleation kinetics were further investigated. Based on the classical nucleation theory, as well as measured induction period and evaluated interfacial tension, the rate of homogeneous nucleation was determined. Higher supersaturation levels result with higher nucleation rates and consequently smaller critical nucleuses were formed at lower energy barriers. According to the evaluated surface entropy factor, it can be assumed that the *cis*-entacapone growth from 2-propanol solution is controlled by the birth and spread mechanism. The obtained prismatic crystal habit is the best from the operational point of view. The temperature range used in this study is in the range of ambient conditions, which is in line with the concept of green chemistry.

Nomenclature

A – constant

AR – aspect ratio

B_0 – nucleation rate, nuclei m^{-2} s^{-1}

CR – cooling rate, K min^{-1}

f – surface entropy factor

ΔG_{cr} – Gibbs free energy for nucleation, J mol^{-1}

k – slope of the straight line defined by eq. 6

k_B – Boltzmann constant, $1.38 \cdot 10^{23}$ J K^{-1}

m_i – mass of dissolved *cis*-entacapone, g

m_c – mass of obtained crystals, g

MZW – metastable zone width, K

n – number of experimental points

N_A – Avogadro constant, $6.022 \cdot 10^{23}$ mol^{-1}

NTU – number of turbidity units

r_c – critical nucleus size, m

R – gas constant, 8.314 J K^{-1} mol^{-1}

S – supersaturation

t_i – induction period, s

t_n – time needed for formation of nucleuses, s

t_g – time needed for growth of nucleuses, s

T – temperature, K

T_s – solubility temperature, K

T_{ss} – supersolubility temperature, K

V – volume, m^3

V_a – volume flow rate of antisolvent, cm^3 min^{-1}

V_m – molar volume, m^3 mol^{-1}

V_s – volume flow rate of solution, cm^3 min^{-1}

x – amount of additive in relation to *cis*-entacapone, %

γ – solution concentration, g dm^{-3}

γ_s – solubility, g dm^{-3}

γ_{ss} – supersolubility, g dm^{-3}

σ – interfacial tension, N m^{-1}

 – standard deviation in eq. 11

References

1. *Myerson, S.,* Handbook of Industrial Crystallization, Butterworth-Heinemann, Woburn, 2002.

2. *Mullin, J. W.,* Crystallization, Fourth edition, Butterworth-Heinemann, Oxford, 2001.

3. *Jones, A. G.,* Crystallization process systems, Butterworth-Heinemann, Oxford, 2002.

4. European Medicines Agency [Internet]. London: European Medicines Agency; 2011 [2011 August 18]. Available from: http://www.ema.europa.eu/

5. *Škalec Šamec, D., Vrbanec, T., Kwokal, A., Šiljković, Z., Šišak, D., Meštrović, E.,* Morphological study of Z-isomer of entacapone, XX. Jubilee Croatian meeting of chemists and chemical engineers, Book of Abstracts, CROATIA, ed. Vasić-Rački Đ, Petrokemija d.d., Kutina, Zagreb, (2007), pp A66.

6. *Kim, K.-J., Mersmann, A.,* Chem. Eng. Sci. **56** (2001) 2315.

7. *Sangwal, K.,* J. Cryst. Growth **318** (2011) 103.

8. *Mersmann, A., Bartosch, K.,* J. Cryst. Growth **183** (1998) 240.

9. *Loffelmann, M., Mersmann, A.,* Chem. Eng. Sci. **57** (2002) 4301.

10. *Kubota, N.,* J. Cryst. Growth **310** (2008) 629.

11. *Kubota, N.,* J. Cryst. Growth **310** (2008) 4647.

12. *Rabesiaka, M., Porte, C., Bonnin-Paris, J., Havet, J.-L.,* J. Cryst. Growth **332** (2011) 75.

13. *Zhu, Y., Youssefb, D., Porte, C., Rannouc, A., Delplancke-Ogletreea, M. P., Lung Somarribab, B., Loi, Mi,* J. Cryst. Growth **257** (2003) 370.

14. *Gherras, N., Fevotte, G.,* J. Cryst. Growth DOI:10.10116/j.jcrysgro.2011.06.058

15. *Wierzbowska, B., Matynia, A., Piotrowski, K., Koralewska, J.,* Chem. Eng. Process **46** (2007) 351.

16. *Trifkovic, M., Sheikhzadeth, M., Rohani, S.,* J. Cryst. Growth **311** (2009) 3640.

17. *Weinberg, M. C., Zanotto, E. D., Manrich, S.,* Phys. Chem. Glasses **33** (1992) 99.

18. *Chenthamarai, S., Jayaraman, D., Ushasree, P. M., Meera, K., Subramanian, C., Ramasamy, P.,* Mater. Chem. Phys. **64** (2000) 179.

19. *Paul, D. P., Thamizhavel, A., Subramanian, C.,* Cryst. Res. Technol. **34** (1999) 503.

20. *Teychene, S., Biscans, B.,* Cryst. Growth Des. **8** (2008) 1133.

21. *Jayalakshimi, D., Sankar, R., Jayavel, R., Kumar, J.,* J. Cryst Growth **276** (2005) 243.

22. *Usharee, P. M., Muralidharan, R., Jayavel, R., Ramasamy, P.,* J. Cryst. Growth **210** (2000) 741.

23. *Tai, C. Y., Chien, W. C.,* Chem. Eng. Sci. **58** (2003) 3233.

24. *Hao, H., Wang, J., Wang, Y.,* J. Cryst. Growth **274** (2005) 545.

25. *Manikowski, A., Larska, Z., Jerkovic, J.,* Process and Product. CROATIA WO 2008/007093A1 (2008).

26. *Garside, J., Mersmann, A., Nyvlt, J.,* Measurement of crystal growth and nucleation rates, IchemE, Salisbury (2002).

27. *Kim, Y., Hyung, W., Haam, S., Gun Shul, Y., Koo, K.-K.,* J. Cryst. Growth **289** (2006) 236.

28. *Zaitseva, N. P., Rashkovich, L. N., Bogatyreva, S. V.,* J. Cryst. Growth **148** (1995) 276.

29. *Šimon, P., Nemčekova, K., Jona, E., Plško, A., Ondrušova, D.,* Thermochim. Acta **428** (2005) 11.

30. *Anastas, P. T., Warner, J. C.* Green Chemistry: Theory and Practice, Oxford University, New York, 1998.